ISSN : 0974 - 7486 Volume 7 Issue 1

Trade Science Inc.

Materials Science

An Indian Journal

Full Paper

MSAIJ, 7(1), 2011 [17-27]

Effect of sulfate ion on silicate ion substitution on hydroxyapatite

N.Y.Mostafa[1,2]*, A.N.Al-Saifi[2], H.A.Azab[2], M.Kamel[2], M.A.Raizk[2]

[1]Chemistry department, Faculty of Science, Taif University, Taif- 888, (KINGDOM OF SAUDI ARABIA)

[2]Chemistry Department, Faculty of Science, Suez Canal University, Ismailia 41522, (EGYPT)

E-mail : nmost69@yahoo.com

Received: 14th August, 2010 ; Accepted: 24th August, 2010

ABSTRACT

Several hydroxyapatite powders were prepared by wet chemical precipitation route at 25°C in presence of different concentration of silicate and sulfate. The powders were characterized using chemical analysis, SEM, XRD and FTIR spectroscopy. The substitution of sulfate ion in the structure of HAP raised silicate substitution up to 9.9 % wt. Increasing silicate and sulfate ions substitutions are associated with increasing carbonate ion substitutions for phosphates and vacancies in the OH^- site. Silicate and sulfate substitution took place via three charge compensation mechanism acting simultaneously. The first is; SiO_4^{4-} group substitute one PO_4^{3-} group and vacancy form in the OH^- site. The second is; SiO_4^{4-} and SO_4^{2-} groups substitute two PO_4^{3-} groups. The third is; SiO_4^{4-} and CO_3^{2-} groups substitute two PO_4^{3-} groups.

KEYWORDS

Hydroxyapatite;
Silicate substitution;
Sulfate substitution;
Crystallinity;
FTIR.

INTRODUCTION

Calcium phosphate compounds are becoming of increasingly great importance in the field of biomaterials[1]. Calcium phosphates are the chemical compounds of a special interest in many interdisciplinary fields of science, including geology, chemistry, biology and medicine[2]. A convenient way to classify calcium phosphate compounds is by groups of definite Ca/P ratios. Generally, various types of calcium phosphates, having different Ca/P ratios from 2.0 to 0.5[3,4], can by synthesized by mixing a calcium and phosphate ion solution under acid or alkaline conditions. TABLE 1 shows various types of synthetic calcium phosphates. The calcium phosphate with the highest Ca/P ratio is hilgenstockite and is represented as $Ca_4O(PO_4)_2$. The calcium phosphate with the lowest Ca/P ratio is monocalcium phosphate monohydrate, the chemical formula of which is $Ca(H_2PO_4)_2.H_2O$ or $Ca(PO_3)_2$. The Ca/P ratios of other calcium phosphates are lower than that of hilgenstockite and higher than that of monocalcium phosphate monohydrate or calcium metaphosphate[3]. Hydroxyapatite ($Ca_{10}(PO_4)_6(OH)_2$, HAP), fluorapatite ($Ca_{10}(PO_4)_6F_2$, FAP) and tricalcium phosphate ($Ca_3(PO_4)_2$, TCP) phases are the common calcium phosphate bioceramics because their chemical composition is similar to that of bone mineral[5-12].

A number of novel processing routes have been developed for preparing fine hydroxyapatite powders, including precipitation[13,14], solid-state reaction[15], sol-

Full Paper

TABLE 1 : Various calcium phosphates

Ca/P	Formula	Name	Abbreviation
2.0	$Ca_4O(PO_4)_2$	Tetracalcium phosphate (Hilgenstockite)	TeCP (TTCP)
1.67	$Ca_{10}(PO_4)_6(OH)_2$	Hydroxyapatite	HAP
	$Ca_{10-x}H_{2x}(PO_4)_6(OH)_2$	Amorphous calcium phosphate	ACP
1.50	$Ca_3(PO_4)_2$	Tricalcium phosphate (α, β, γ)	TCP
1.33	$Ca_8H_2(PO_4)_6.5H_2O$	Octacalcium phosphate	OCP
1.0	$CaHPO_4.2H_2O$	Dicalcium phosphate dehydrate (Brushite)	DCPD
1.0	$CaHPO_4$	Dicalcium phosphate (Monetite)	DCP
1.0	$Ca_2P_2O_7$	Calcium pyrophosphate(α,β,γ)	CPP
1.0	$Ca_2P_2O_7.2H_2O$	Calcium pyrophosphate dihydrate	CPPD
0.7	$Ca_7(P_5O_{16})_2$	Heptacalcium phosphate (Tromelite)	HCP
0.67	$Ca_4H_2P_6O_{20}$	Tetracalcium dihydrogen phosphate	TDHP
0.5	$Ca(H_2PO_4)_2.H_2O$	Monocalcium phosphate monohydrate	MCPM
0.5	$Ca(PO_3)_2$	Calcium metaphosphate(α,β,γ)	CMP

gel syntheses[16-19], hydrothermal reactions[20,21], emulsion and microemulsion syntheses[22,23], mechanochemical syntheses[24-27], and a combination of mechanochemical and hydrothermal[28] and ultrasonically assisted reaction[29]. Depending on the techniques used, HAP with various morphologies, specific surface, composition, and crystalline degree have been obtained and shown to have different effects on the bioactivity, mechanical properties and dissolution behavior in biological environment[30-32]. The most commonly used technique for the formation of HAP powder is the wet methods in aqueous solutions both by simple preciptation method[30,33] or hydrolysis of acidic calcium phosphate salts[34-36].

Hydroyapatite crystal structure can be modified with varieties of ion substitutions[37]. The list of possible additives includes (but is not limited to) the following cations: Na^+, K^+, Mg^{2+}, Ca^{2+}, H^+ and anions: PO_4^{3-}, HPO_4^{2-}, $H_2PO_4^-$, CO_3^{2-}, HCO_3^-, SO_4^{2-}, HSO_4^-, Cl^-, F^-, SiO_4^{4-} [38]. The incorporation of these substituents affects the mechanisms of formation, the stabilities, the morphologies, and the solubility of hydroxyapatite crystals[39].

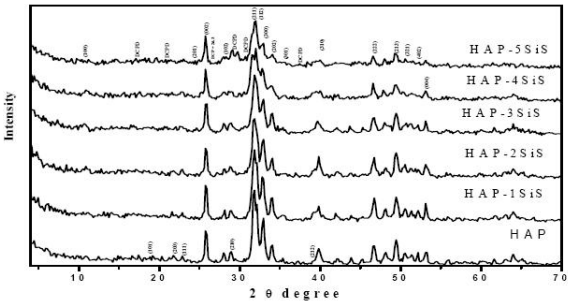

Figure 1 : XRD patterns of hydroxyapatite powder dried at 105°C for 24 hours

Both experimental and theoretical research have been tried to solve the complexity of these types of substitutions[40,41]. However, the types and extents of most of these substitutions are incompletely understood because of many practical complications. One of these complications is the difficulty in establishing the mechanisms of charge compensations due to coupled and multiplied substitutions[42].

Although the existence of natural silicophosphates, silicosulfo-phosphates and silicosulfate apatites is known, only limited synthesis studies have been reported[43]. Both silica and sulfur are found as trace elements in human hard tissue[44]. Also, carbonate substitutions are labeled as A- and B-type, depending on whether they occupy the OH^- or PO_4^{3-} sites in the hydroxyapatite, respectively[45,46]. Substitutions of carbonate groups in phosphate positions are observed in human bone mineral[47]. The role of silicates substitutions in the hydroxyapatite lattice is important with respect to physicochemical properties and bioactivity[42].

Studies carried out by Carlisle[48,49] indicated the importance of the silicon on bone formation and calcification. Recently, it has been observed that the addition of Si during the HAP synthesis leads to an improvement of the bioactive behavior[50,51]. It means that the implant is able to join chemically to the bone through a strong "bioactive bond". In this way, the osteointegration and the good performance of the implant are ensured[52,53]. Silicon substitutions in HAP have been studied by many investigators, but no one have determined the maximum extent of substitution[42].

The aim of this research is to prepare and characterize several silicate and sulfate substituted hydroxyapatite powders (HAP-SiS) using silicic acid (H_4SiO_4) and sulfuric acid as a precursors of silicate and sulfate, respectively, under N_2 gas to prevent CO_2 contamina-

tion. There was expected that sulfate substitution will increase the amount of silicate substitution in hydroxyapatite structure.

MATERIALS AND METHODS

Pure $CaCO_3$ powder was heated at 1100°C for 4 hours, and the resultant CaO powder was used as it is. All the other chemicals were analytical grades. Hydroxyapatite powders were prepared by aqueous precipitation method. The precipitation was carried out in a polyethylene bottle close under N_2 gas at room temperature. Precipitations were carried out by titrating 1000 mL suspension of $Ca(OH)_2$ (0.200 M) simultaneously with 500 mL solution of H_3PO_4, 500 mL H_4SiO4 and 500 mL H_2SO_4 based on the methods described elsewhere[42]. Five grades of silicate and sulfate–substituted hydroxyapatite (HAP-SiS) powders were synthesised by maintaining the Ca/(P+Si+S) ratios fixed at 1.67, as shown TABLE 2 which shows the expected chemical composition (% wt), expected molar ratios and formulas of different silicate and sulfate co-substituted hydroxyapatite. All the preparations of hydroxyapatite were dried at 105°C for 24 hours.

The chemical analysis was measured by X-ray fluorescence (XRF). The carbonate content was determined by CHN analysis using a Perkin Elmer 2400 CHN analyser.

X-ray diffraction (XRD) analysis was performed using an automated diffractometer (Philips type: PW1840), at a step size of 0.02°, scanning rate of 2° in 2θ/min., and a 2θ range from 4° to 60° The values of full width at half-maximum of (FWHW) of the peak of the (002) plane, representative of the crystallites along the c axis, and of the peak of the (300) plane, representative of the crystallites along the a axis, were used in the calculation according Scherrer's formula[54].

$$D = K\lambda/[\beta_{1/2}\cos\theta]$$

where D is the crystallite size in A°, K is Schrrer constant (0.89), λ is the wavelength of X-rays beam(1.5405 A°), θ is the diffraction angle (12.92) for the reflection (002) and (16.45) for reflection (300), and $\beta_{1/2}$, is defined as the diffraction peak width at half maximum height, expressed in radian.

The powders morphology was investigated using SEM (JOEL, Model: JSM-5600, Japan.) equipped with secondary electron detector and EDX. All samples were coated with gold. FTIR spectroscopic measurements were carried out using a spectrometer (FTIR, JASCO 470). The samples were mixed with KBr with a sample/KBr weight ratio of ~1/100 and compressed to give self-supporting pellets.

RESULTS

Characterization

XRD Diffractograms of HAP-SiS powders as shown in figure 1, revealed no secondary phases, such as tricalcium phosohate (TCP), tetracalcium phosphate (TTCP), or calcium oxaide (CaO) besides hydroxyapatite phase on the basis of JCPDS Card No. 9-432[55] in samples from HAP to HAP-4SiS. Reflections of the silicon and sulfate–containing hydroxyapatites (HAP-SiS) are in general broader than those of the pure hydroxyapatite (HAP). In sample HAP-5SiS, the maxima are characteristic to (002), (300), (212) and (202) reflections. Similar results have been observed for HAP-Si coatings obtained via sputtering deposition[56] or sol-gel coating[57]. This indicates a decrease of crystallinity with the increasing of silicate and sulfate contents, which could be attributed to different charge compansetion mechanisum for isomorphous substitution of PO_4^{3-} by SiO_4^{4-}, and SO_4^{2-}. However, the broadening of the XRD peaks could result from an effective decrease in the crystallite size. As being previously observed in other study[58].

XRD data of HAP-5SiS sample indicates to the formation of dicalcium phosphate dihydrate (brushite) on the basis of JCPDS Card No. 72-0713 as minor phase beside hydroxyapatite. The formation of this phase may be attributed to decrease in the amount of phosphate with respect to amount of calcium as confirmed by Ca/P of 3.615 for sample HAP–5SiS as shown by XRF analysis Table 3. It was found that drops in P concentration were related to the formation of brushite, $CaHPO_4.2H_2O$[59]. Oliveira et al.[60] was found that a gradual reduction of HAP crystals simultaneously with the growth of brushite crystals, until the complete HAP disappearance. Also, it could be expected that increased Si amount would cause HAP crystals to be more soluble, releasing more Ca^{2+} and P^{5+} ions into the culturemedium; thus rapidly re-precipitating and devel-

oping a newly formed CaP-rich[61,62].

The crystal sizes as determined using Scherrer's equation along a crystallographic axis and along c crystallographic axis are shown in TABLE 3. The crystal size for all HAP-SiS samples except HAP-3SiS along a axis decreases with the increases of silicate and sulfate contents, while the crystal size along c axis increases with the increase of silicate and sulfate contents. The crystal size for HAP-3SiS sample along a axis and along c axis is increased and decreased respectively. Silicon substitution results in a decrease in the a axis, an increase in the c axis of the unit cell of hydroxyapatite and a slight decrease in the actual unit volume[58]. Rouse and Dunn[63] noted that, the Si:S ratio is essentially constant at 1:1 and the mean of the effective radii of SiO_4^{4-} and SO_4^{2-} is equal to the effective radius of PO_4^{3-}. Thus changes in the (Si, S): P ratio should not affect the size o f the unit cell. Carbonate groups in a precipitated hydroxyapatite was known to cause a reduction in a axis and a slight increased in c axis values related to the stoichiometric ones[31,64], while systematic decrease in carbonate content as the principal causes of the increase in a axis and c axis[63]). The change of the lattice constants of ion substituted hydroxyapatite clearly demonstrates that silicate and sulfate ions are structurally incorporated, they do not just cover the surface of hydroxyapatite. The presence of SO_4^{2-} and silicate reduce the growth of (100) and (010) and inhance the growth of (001) face. The products consisted of uniform apatite phase and had the XRD reflections characteristic of the (100), (200) and (300) planes. These results indicate that the present apatite gives preferred orientation in the c axis direction of the hexagonal crystal, leading to develop the a or b plane of the apatite crystal[65].

Generally the aspect ratios (length/diameter) increase with increasing sulfate and silicate contents, the range of 1.5-3.1.

Chemical composition of the HAP powder is one of the most crucial parameters in determining different properties like solubility, thermal stabilities and sintering properties[5]. The chemical compositions determined by using XRF and CHN analysis of all samples are given in TABLE 2 and TABLE 3. The contents of silicon, sulfure, calcium and phosphorus are smaller than those present in the initial mixes. This implies that some of silicate, sulfate and phosphate ions remained in the mother liquor solution after precipitation. Incorporation of carbonate ions from the atmosphere also contributes to the decrease in Si, S, P and Ca contents in the final powders. The most notable effect is the increase of carbonate contents as the silicate contents increase[66]. Carbonates are usually, observed in HAP powders[37,58] and coatings[57] deposited by the sol-gel technique. Sprio et al.[67] have been stated that there was a competition between SiO_4^{4-} and CO_3^{2-} for substitution in PO_4^{3-} position. While in the present investigation, silicate and sulfate ions substitutions induce carbonate ions co-substitutions which was dissolved from atmosphere.

The Ca/P molar ratio is one of the important characteristics of the biomaterial to be used for bone substitution, because of scaling its phase purity, chemical homogeneity, and solubility[68]. Therefore, the Ca/P molar ratio of the all samples were determined by XRF, it was found to be 1.66 for HAP sample, which is quite similar to that of pure HAP (1.67). The slight increase in the Ca/P ratio for other samples can be attributed to the substitution of silicate, sulfate and carbonate into apatite, indicating the formation of anion substituted-HAP. It also shows that the amount of CO_3^{2-} substitution is very low. The calculated Ca/(P+Si+S) ratio of samples from HAP–1SiS to HAP–4SiS is ranged from 1.52 to 1.65 appreciable and fits quite well with that of calcium deficient hydroxyapatite[69]. While, the deviation of the value of Ca/(P+Si+S) for sample HAP-5SiS is attributed to the formation of brushite as a secondary phase beside hydroxyapatite.

Comparing the expected chemical composition in TABLE 2 and the found chemical composition in TABLE 3. The found sulfur, phosphorous and calcium are lower than expected. However silicon contents are higher than expected. These are due to the higher solubility of $CaSO_4$ which causes lose of Ca^{2+} and SO_4^{2-} in the mother liquor. Comparing the maximum amounts of silicon with previous study conducted with the same group[42], we found a high silicon percent in the present results.

Microstructure of samples HAP, HAP-3SiS and HAP-5SiS did not show any differences between Si-substituted and unsubstantiated hydroxyapatite. All powders consist of hard sub micrometer agglomerates

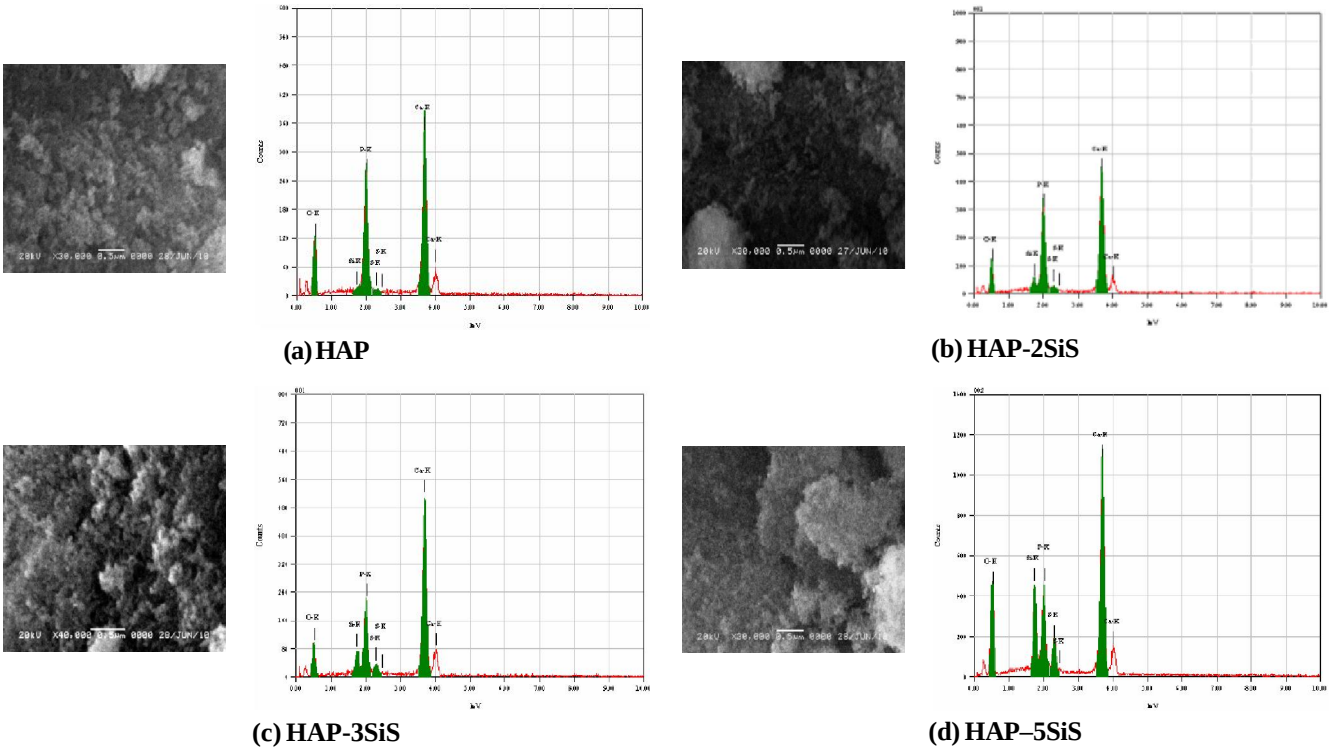

Figure 2 : Scanning electron micrographs and EDS plots of; (a) HAP, (b) HAP-2SiS, (c) HAP-3SiS and (d) HAP–5SiS

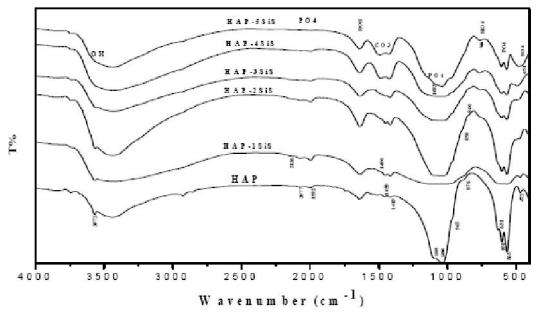

Figure 3 : FTIR spectra of different hydroxyapatite powders dried at 105°C for 24 hours

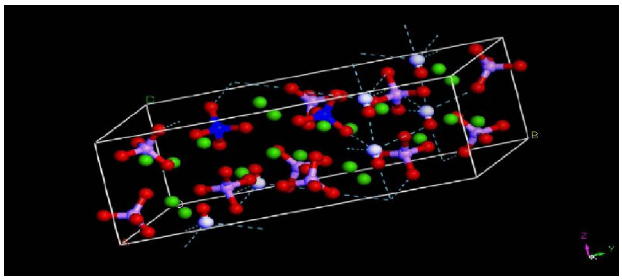

Figure 4 : The bent hydrogen bond between O-H and silicate group (O-H- - -$SiPO_3$) Si=blue, H=white, O=red, Ca=green and P=**

which are composed of fine crystallites. Generally, these agglomerate particles are hard to break down even with long time ultrasonication. However, EDS analyses, as shown also in figure 2, clearly depict the progress of increasing silicate and sulfate contents of samples HAP, HAP-2SiS, HAP-3SiS and HAP-5SiS.

FTIR spectroscopy

FTIR spectroscopy was used to study the types of constituting groups in the synthezied hydroxyapatite and substituted hydroxyapatite powders. The effect of the substituted ions namely; silicon (Si), sulfure (S), and carbonate (CO_3^{2-}) on the different functunal groups; such as hydroxyl and phosphate groups, of hydroxyapatite has been verified. In addition, the position of the carbonate ion whether in the phosphate (B) and/ or hydroxyl (A) sites in the different apatite powders, was determined.

Valuable information on the short-range ordering in materials can be obtained by infrared absorption (FT-IR) spectra. Figure 3, depicts FT-IR spectra of synthesized hydroxyapatite and substituted hydroxyapatite powders dried at 105°C for 24 hours. All spectra possess a broad band at 3400-3200 cm^{-1}, due to stretching vibrations of O-H groups in adsorbed H_2O. This broadening is due to the formation of hydrogen bonding with a wide range of strengths[70,71]. It is well known that as hydrogen bonding strength increases,

Full Paper

TABLE 2 : Expected chemical composition (% wt), and formulas of different silicate and sulfate co-substituted hydroxyapatite (HAP-SiS)

Sample	Formulas	%Ca	%P	%Si	%S	Predicted [Ca/(P+Si+S)]
HAP	$Ca_{10}(PO_4)_6(OH)_2$	39.8939	18.499	0	0	1.67
HAP-1SiS	$Ca_{10}(PO_4)_{5.905}(SiO_4)_{0.0475}(SO_4)_{0.0475}(OH)_2$	39.8973	18.2	0.1328	0.1516	1.67
HAP-2SiS	$Ca_{10}(PO_4)_{5.4}(SiO_4)_{0.3}(SO_4)_{0.3}(OH)_2$	39.915	16.657	980.8391	550.95804	1.67
HAP-3SiS	$Ca_{10}(PO_4)_5(SiO_4)_{0.5}(SO_4)_{0.5}(OH)_2$	39.929	615.42967	1.399	1.5973	1.67
HAP-4SiS	$Ca_{10}(PO_4)_4(SiO_4)(SO_4)(OH)_2$	39.9654	12.3548	2.8007	3.19749	1.67
HAP-5SiS	$Ca_{10}(PO_4)_2(SiO^4)_2(SO_4)_2(OH)_2$	40.037	6.18848	5.61147	6.40647	1.67

TABLE 4 : CHN analysis of different silicate and sulfate-substituted hydroxyapatite (HAP-SiS) powderes

Sample	% C	% H
HAP	0.07	0.64
HAP-1SiS	0.35	0.72
HAP-2SiS	0.27	0.76
HAP-3SiS	0.57	0.73
HAP-4SiS	0.44	0.97
HAP-5SiS	0.60	0.95

TABLE 3 : Crystallite sizes along a axis and along c axis of different hydroxyapatite

Sample	Crystallite size along a-axis (nm)	Crystallite size along c-axis (nm)	Aspect ratio
HAP	31.1	47.4	1.52
HAP-1SiS	28.7	48.9	1.70
HAP-2SiS	27.6	49.7	1.80
HAP-3SiS	26.7	41.7	1.57
HAP-4SiS	17.9	55.7	3.11
HAP-5SiS	18.8	50.4	2.68

TABLE 5 : Chemical analysis (% wt.) and molar ratios of different silicate and sulfate-substituted hydroxyapatite (HAP-SiS) powderes

Sample	% Ca	% P	% Si	% S	Ca/P	Ca/P+Si+S
HAP	37.74	17.52	0	0	1.665	1.665
HAP-1SiS	37.46	17	0.407	0.0801	1.703	1.652
HAP-2SiS	35.835	16.2	1.44	0.425	1.710	1.522
HAP-3SiS	35.32	14.8	2.16	0.681	1.844	1.531
HAP-4SiS	34.44	10.9	4.4	1.51	2.441	1.547
HAP-5SiS	30.08	6.43	9.92	2.13	3.615	1.197

the stretching vibrations frequency of O-H group decreases[72]. The bending vibration band of molecular H_2O appears at 1632 cm^{-1}. The bands at 1400-1550 cm^{-1} is assignable to CO_3^{2-}[73].

The strong bands in the wavenumber range 900-1200 cm^{-1}, correspond to P-O stretching vibration modes of the phosphate groups. The doublet bands at 603-565 cm^{-1} correspond to the O-P-O bending mode. The bands at 3572 and 631 cm^{-1} correspond to the stretching and bending modes, respectively, of the hydroxyl groups in hexagonal channels.

Comparing the FT-IR spectra of different hydroxyapatites, there are some systematic changes in phosphate, hydroxyl, carbonate, sulfate and silicate. These group of bands will be discussed separately for convince.

Phosphate bands

The spectral range 900-1200 cm^{-1} contains the symmetric and the asymmetric P-O stretching modes of the phosphate groups. It is well known that for hydroxyapatite, the symmetric P-O stretching mode occurs at 964 cm^{-1}, while the asymmetric stretching modes occur at 1036 and 1095 cm^{-1}[37,74]. As shown in figure 3, the infrared symmetric and the asymmetric P-O stretching bands of phosphate groups decrease and become less resolved as the silicate and sulfate contents are increased in all the samples[37,74]. Sample HAP-5SiS is excluded from this observation due to the formation of secondary phases[75]. Similar changes were also observed in the doublet at 603-565 cm^{-1}, corresponds to the anti-symmetric bending motion of phosphate groups[37,74].

The group of weak intensity bands at the wavenumber range of 2200 cm^{-1} to 1950 cm^{-1} region derives from overtones and combinations of the ν_3 and ν_1 PO_4 modes[15,76]. The sharpness of bands, especially sharpness of the 631 cm^{-1}, 601 cm^{-1}, and 574 cm^{-1} bands, indicate a well-crystallized HAP[74]. However, both, stretching and bending bands positions of phosphate groups are quite obviously unaffected by the silicate substitution.

Carbonate bands (CO_3^{2-})

The carbonate bands appear in all samples at wavenumbers 1468-1418 cm^{-1} and 875 cm^{-1}, correspond to the CO_3^{2-} groups substituting for phosphate groups in the apatite structure[37]. These correspond to a B-type carbonate-hydroxyapatite, similar to biological apatites[71]. As seen in figure 3, the CO_3^{2-} bands intensify as the silicate contents increases. This was confirmed by CHN analysis (TABLE 3.2).

Hydroxyl bands

The most notable effect of silicate substitution on

TABLE 6 : The effect of silicate and sulfate substitution on the O-H vibration wavenumber

Sample	HAP	HAP-1SiS	HAP-2SiS	HAP-3SiS	HAP-4SiS	HAP-5SiS
Stretching(cm^{-1})	3572	3568	3567.5	3564	3560	
Shift(cm^{-1})	N/A	-4	-3.5	-8	-12	
Bending(cm^{-1})	632.5	625				
Shift(cm^{-1})	N/A	-7.5				

FT-IR spectra of hydroxyapatite is the change in the hydroxyl stretching band at 3572 and bending band at 631 cm^{-1}. In figure 3, intensities at 3572 and 631 cm^{-1} of silicate and sulfate substituted samples decrease with increasing silicate and sulfate substitution level and both bands nearly disappear for sample HAP-4SiS. Many investigators[58,77-79] have been accounted this due to the charge compensation mechanism in which HAP unit cell loss one OH group for every silicate substituted from phosphate.

Another remarkable effect of silicate substitution is the negative shifts on both O-H stretching and bending bands, as shown in TABLE 3.3. These negative shifts increase with increasing silicate and sulfate contents. It is well known that, the shift in O-H bands is a marker for hydrogen bonding. Hydroxyl groups capable of two types of hydrogen bonding in hydroxyapatite structure. O-H makes hydrogen bonding with other O-H in the same hexagonal channels[15]. Stronger hydrogen bond formation of the type O-H- - -O-H is usually associated with downward shift in the O-H stretching band and upward shift in O-H bending band[15]. However, in the present case both O-H stretching and bending bands show downward shift. Thus, this type of hydrogen bonding is not responsible for the observed shift in O-H vibrations. Increasing silicate substitution accompanied by a decrease of the O-H contents which will also debilitate O-H- - -O-H hydrogen bonding[15,80].

The second type of weak hydrogen bonding is commonly observed between O-H and the closest oxygen of the three phosphate groups, which surround the O-H ion[81]. An O-H- - -O-PO_3 hydrogen bonding, would be bent because of the O-H bond direction along the c axis; however, bent O-H- - -O-PO_3 bonds are common hydroxyapatites[82]. The wavenumber of O-H vibration band is different for HAP (3572 cm^{-1}) and HAP-3SiS (3564 cm^{-1}) (TABLE 3.4). These values point out a stronger hydrogen bond in the silicate substituted hydroxyapatite than for unsubstituted hydroxyapatite. This attributes to the difference between O-Si and O-P bonds in both polarity and length. Thus, silicate ions are capable of forming stronger hydrogen bonding with O-H group than phosphate ions[83]. DFT (density functional theory) calculations of Astala et al.[83] have been indicated that the PO_4 group has a weaker affinity for H than the SiO_4. Figure 3.4 shows the bent type strong hydrogen bonding between O-H and silicate group (O-H- - -O-$SiPO_3$).

Silicate bands

It is well known that, the most intense spectral features of silicates appear as a complex group of bands in the range of 1100-900 cm^{-1}, are attributed to asymmetrical stretching vibrations of SiO_4 tetrahedra[84]. The second most intense silicate bands are broadly characterized as O-Si-O deformation or bending modes, which occur in the 556-400 cm^{-1} region. Figure 3.3, clearly shows that the stretching vibration bands of silicate interfere with phosphate stretching vibration bands, resulting in the observed broadening of the later with increasing silicate substitutions. The band at 766 cm^{-1} is observed in all hydroxyapatites containing silicate and its intensity progressively increases as silicate contents increases[85]. Starz et al.[86] relate the bands at 750-810 cm^{-1} to the presence of a combination of vibrations of Si-O-Si, Si-O-P and P-O-P bridges.

It is common to see additional peaks in silicate substituted hydroxyapatites. Gibson et al.[78] was able to detected peaks at 945, 890 and 840 cm^{-1} for hydroxyapatite powder with a 0.4 % wt. of Si. According to those findings, the presence of a peak at 945 cm^{-1} could justify the broadening of the 960 cm^{-1} band observed in silicate substituted hydroxyapatites. In figure 3.2, two new (shoulder shaped) bands at 931 and 892 cm^{-1} occur. Tanizaw et al.[87] have been also related these bands to the presence of silicate in the apatite structure.

Yu et al.[88] was able to assign band at 811 cm^{-1} due to Si-O stretching of dimmer silicate chains. This band appears very week in sample HAP-2SiS and HAP-3SiS at 828 cm^{-1} and increases with increase silicate substitution, indicating silicate polymerization.

Sulfate bands

The SO_4^{2-} ion possesses tetrahydral symmetry[89] with four active fundamentals in the inferared, ν_1 at 981

cm^{-1}, ν_2 at 451 cm^{-1}, ν_3 at 1104 cm^{-1}, and ν_4 at 613 cm^{-1}. Only the absorption band at 456 cm^{-1} appears very weak in spectrum of sample HAP-5SiS, confirms the presence of ν_1 SO_4^{2-} and the other three bands are interfere with the phosphate bands.

DISCUSSION

Hydroxyapatite prepared in absence of silicate and sulfate ions (HAP) incorporates minor amount of CO_3^{2-} in its lattice. FTIR spectroscopy showed that carbonate ions substitute for phosphate ions (B-type hydroxyapatite). The chemical analysis of HAP sample suggested that the most probable charge compensation took place with the following mechanism[70];

$$Ca^{2+} + 2PO_4^{3-} \rightarrow V_{Ca2+} + 2CO_3^{2-} \quad (1)$$

where, V_{Ca2+} represents a vacancy in site occupied by Ca^{2+} ions. This conclusion is also supported by thermal stability of this sample at 1100°C. Decomposition of calcium deficient hydroxyapatite starts at 900°C to form tricalcium phosphate[5]. However, carbonate ions substitutions stabilize the HAP powder at high temperatures (1100°C). The increase in carbonate content increases the Ca/P ratio (TABLE 3.2 and 3.3). When the carbonates are removed at high temperature (900°C), the HAP phase is rendered more stable, due to the increase of Ca/P ratio over the stoichiometric ratio (1.67)[84].

The decrease in O-H stretching and bending bands intensities with increasing silicate content, indicates the decrease of the hydroxyl content as the degree of substitution increases. X-ray and neutron diffraction studies[51,90] have shown that silicate ions replace phosphate ions. Thus, the extra negative charge of the SiO_4^{4-} groups is compensated by formation of vacancies at the OH^- sites. This suggests the first charge compensation mechanism for silicate substitution, to be as follows:

$$PO_4^{3-} + OH^- \rightarrow SiO_4^{4-} + V_{OH^-} \quad (2)$$

where V_{OH-} represents a vacancy in site occupied by OH^- ion. If this is the only working mechanism, the composition of the powders could be described by the formula; $Ca_{10}(PO_4)_{6-y}(SiO_4)_y(OH)_{2-y}$. Dunfield et al.[91] have reported that, at doping level above 0.2 mole SiO_2/mole hydroxyapatite, the stretching mode falls to zero, for samples prepared at controlled conditions without carbonates. However, in the present investigation, the stretching mode of OH is detected up to 1.48 mole SiO_2/mole hydroxyapatite (sample HAP-3SiS). This points out that the pervious charge compensation mechanism cannot account for all silicate substitutions. In the present study, the chemical analysis and the FTIR spectra show that sulfate groups in phosphate sites increases as silicate contents increases. This suggests that the second charge compensation proceeds according to the following mechanism:

$$2PO_4^{3-} \rightarrow SiO_4^{4-} + SO_4^{2-} \quad (3)$$

Considering only the previous substitution mechanism, the composition of the powders could be described by the formula; $Ca_{10}(PO_4)_{6-2z}(SiO_4)_z(SO_4)_z(OH)_2$. When the number of moles of sulfate is equal to that of silicate, no hydroxyl vacancies will be created.

Some authors[57,79] observed that the amount of carbonate ions increases with the $Si(OCH_2CH_3)_4$ addition. They suggested that the competition between SO_4^{2-} and SiO_4^{4-} groups for the phosphate sites causes some of the silicate to stay free without being incorporated into the hydroxyapatite. However in the present study, the chemical analysis and the FT IR spectra show that all the powders (with and without Si) contain carbonate groups in phosphate sites and carbonate content increases as silicate contents increases.

$$2PO_4^{3-} \rightarrow SiO_4^{4-} + CO_3^{2-} \quad (4)$$

This type of charges compensation are expected to be similar to happen in part in the formation of bone. Assuming that only the mechanical structure can be formulated in general as follows: $Ca_{10}(PO_4)_{6-2z}(SiO_4)_z(CO_3)_z(OH)_2$.

CONCLUSIONS

Hydroxyapatite powder pure and several silicate and sulfate substituted hydroxyapatite powders (HAP-SiS) were successfully prepared by wet chemical precipitation route using silicic acid (H_4SiO_4) and sulfuric acid as precursors of silicate and sulfate, respectively, under N_2 gas to prevent CO_2 contamination at room temperature. The introduction of sulfate ion in the structure of HAP raised the percentage of silicate up to 9.9 % wt. Si. Increasing substitution of SiO_4^{4-} and SO_4^{2-}

for PO_4^{3-} is accompanied by increase of CO_3^{2-} substitutions for PO_4^{3-} and decrease of OH^- contents in hydroxyapatite crystal structure. Incorporation of carbonate ions from the atmosphere also contributes to the decrease in Si, S, P and Ca contents in the final powders. While the competition between SO_4^{2-} and SiO_4^{4-} groups for the phosphate sites causes some of the sulfate ions to stay free without being incorporated into the hydroxyapatite in the HAP-5SiS sample. Although powder crystallinity is strongly reduced as the extent of the substitution increases, but there are no signs exist where the apatite structure collapses and an amorphous phase forms.

ACKNOWLEDGMENT

Suez Canal University is acknowledged for providing the laboratory facilities for the preparations.

REFERENCES

[1] M.S.Dojsic, V.B.Miskovic-Stankovic, Z.M.Kacarevic-Popovic, B.M.Jokic, N.Bibic, M.Mitric, S.K.Milonjic, R.Jancic-Heinemann, J.Stojanovic; Eng.Aspects, **341**, 110-117 **(2009)**.

[2] S.Koutsopoulos; J.Biomed.Mater.Res., **62(4)**, 600-612 **(2002)**.

[3] H.Aoki; 'Science and Medical Applications of Hydroxyapatite', Takayama Press, Tokyo, **(1991)**.

[4] S.Koutsopoulos, A.Kontogeorgou, J.Petroheilos, E.Dalas; J.Mater.Sci.Mater.Med., **9**, 421-424 **(1998)**.

[5] N.Y.Mostafa; Materials Chemistry and Physics, **94**, 333-341 **(2005)**.

[6] N.Bouslama, F.Ben Ayed, J.Bouaziz; Journal of the Mechanical Behavior of Biomedical Materials, **3(1)**, 2-13 **(2010)**.

[7] C.X.Wang, X.Zhou, M.Wang; Materials Characterization, **52(4-5)**, 301-307 **(2004)**.

[8] C.Liou Sz, S.Y.Chen; Biomaterials, **23**, 4541-4547 **(2002)**.

[9] F.Ben Ayed, J.Bouaziz; Ceramics Int., **34(8)**, 1885-1892 **(2008)**.

[10] F.Ben Ayed, J.Bouaziz; J.Eur.Ceram.Soc., **28(10)**, 1995-2002 **(2008)**.

[11] N.Bouslama, F.Ben Ayed, J.Bouaziz; Ceramics International, **35**, 1909-1917 **(2009)**.

[12] K.Chaari, F.Ben Ayed, J.Bouaziz, K.Bouzouita; Materials Chemistry and Physics, **113(1)**, 219-226 **(2009)**.

[13] S.Puajindanetr, S.M.Best, W.Bonfield; Brit.Ceram.Trans, **93(3)**, 96-99 **(1994)**.

[14] A.Lopez-Macipe, R.Rodriguesz-Clements, A.Hidalgo-Lopez, L.Arita, M.V.Garcia-Garduno, E.Rivera, V.M.Castano; J.Mater.Synth.Process, **6(1)**, 21-6 **(1998)**.

[15] B.O.Fowler; Inorg.Chem., **13(1)**, 194-207 **(1974)**.

[16] J.Klinkaewnarong, E.Swatsitang, C.Masingboon, S.Seraphin, S.Maensiri; Current Applied Physics, **10**, 521-525 **(2010)**.

[17] G.Bezzi, G.Celotti, E.Landi, T.M.G.La Torretta, I.Sopyan, A.Tampieri; Mater.Chem.Phys., **78**, 816-824 **(2003)**.

[18] T.Anee Kuriakose, S.Natayana Kalkura, M.Palanichamy, D.Arivuoli, G.Karsten Dierks, G.Bocelli, C.Betzel; J.Cryst.Growth, **263**, 517-523 **(2004)**.

[19] R.Nemoto, S.Nakamura, T.Isobe, M.Senna; J.Sol-Gel Sci.Technol., **21**, 7-12 **(2001)**.

[20] H.Hattori, Y.Iwadate; J.Am.Ceram.Soc., **73(6)**, 1803-1805 **(1990)**.

[21] M.Yoshimura, H.Suda, K.Okamoto, K.Ioku; J.Mater.Sci., **29(13)**, 3399-3402 **(1994)**.

[22] M.G.S.Murray, J.Wang, C.B.Ponton, P.M.Marquis; J.Mater.Sci., **30(12)**, 3061-3074 **(1995)**.

[23] G.K.Lim, J.Wang, S.C.Ng, L.M.Gan; Mater.Lett., **28**, 431-436 **(1996)**.

[24] W.Kim, Q.Zhang, F.Saito; J.Mater.Sci., **35(21)**, 5401-5405 **(2000)**.

[25] K.C.B.Yeong, J.Wang, S.C.Ng; Biomaterials, **22(20)**, 2705-2712 **(2001)**.

[26] S.H.Rhee; Biomaterials, **23(4)**, 1147-1152 **(2002)**.

[27] B.Yeong, X.Junmin, J.Wang; J.Am.Ceram.Soc., **84(2)**, 465-467 **(2001)**.

[28] W.L.Suchanek, P.Shuk, K.Byrappa, R.E.Riman, K.S.Tenhuisen, V.F.Janas; Biomaterials, **23(3)**, 699-710 **(2002)**.

[29] Y.Fang, D.K.Agrawal, D.M.Roy, R.Roy, P.W.Brown; J.Mater.Res., **7(8)**, 2294-2298 **(1992)**.

[30] R.E.Riman, W.L.Suchanek, K.Byrappa, C.W.Chen, P.Shuk, C.S.Oakes; Solid State Ionics, **151**, 393-402 **(2002)**.

[31] I.R.Gibson, W.Bonfield; J.Biomed.Mater.Res., **59**, 697-708 **(2002)**.

[32] V.P.Orlovskii, V.S.Komlev, S.M.Barinov; Inorganic Materials, **38(10)**, 973-984 **(2002)**.

[33] Y.Liu, W.Wang, Y.Zhan, C.Zheng, G.Wang; Mater.Lett., **56(4)**, 496-501 **(2002)**.

[34] K.S.TenHuisen, P.W.Brown; Biomaterials, **19(23)**, 2209-2217 **(1998)**.

[35] R.I.Martin, P.W.Brown; J.Biomed.Mater.Res.A, **35(3)**, 299-308 **(1997)**.

[36] P.W.Brown, R.I.Martin, K.S.TenHuisen; Am.Ceram.Soc., Westerville, OH, 37-48 **(1996)**.

[37] J.C.Elliott; 'Structure and Chemistry of the Apatites and Other Calcium Orthophosphates', Studies in Inorganic Chemistry 18, Elsevier Science, Amsterdam, **(1994)**.

[38] F.C.M.Driessens, J.A.Planell, M.Boltong, I.Khairoun, M.P.Ginebra; J.Eng.Med., **212**, 427-435 **(1998)**.

[39] K.S.Leshkivich, E.A.Monroe; J.Mater.Sci., **28**, 9-14 **(1993)**.

[40] S.Peroos, Z.Du, N.H.de Leeuw; Biomaterials, **27**, 2150-2161 **(2006)**.

[41] N.Y.Mostafa, P.W.Brown; Journal of Physics and Chemistry of Solids, **68**, 431-43 **(2007)**.

[42] N.Y.Mostafa, H.M.Hassan, F.H.Mohamed, H.Omar; Materials Research Bulletin, doi:10.1016/j.materresbull.2009.11.013, **(2008)**.

[43] K.S.Leshkivich, E.A.Monroe; J.Mater.Sci.: Mater.In Med., **4**, 86-94 **(1993)**.

[44] F.Losee, T.W.Cutress, R.Brown; 'Trace Elements in Human Dental Enamel', In Trace Substances in Environmental Health 7, D.D.Hemphill, Ed.; University of Missouri, Columbia, 19 **(1973)**.

[45] M.E.Fleet, X.Liu; J.Solid State Chem., **177**, 3174-3182 **(2004)**.

[46] Y.Suetsugu, Y.Takahashi, F.P.Okamura, J.Tanaka; J.Solid State Chem., **155**, 292-297 **(2000)**.

[47] A.Kaflak-Hachulska, A.Samonson, W.Kolodziejski; Calcif.Tissue.Int., **73**, 476-486 **(2003)**.

[48] E.M.Carlisle; Science, **167(916)**, 279-280 **(1970)**.

[49] E.M.Carlisle; Calc.Tissue Int., **33**, 27-34 **(1981)**.

[50] A.E.Porter, N.Patel, J.N.Skepper, S.M.Best, W.Bonfield; Biomaterials, **24**, 4609-4620 **(2003)**.

[51] D.Arcos, J.Rodríguez-Carvajal, M.Vallet-Regí; Solid State Sciences, **6**, 987-994 **(2004)**.

[52] L.L.Hench; J.Am.Ceram.Soc., **74(7)**, 1487-1510 **(1991)**.

[53] H.Oonishi, L.L.Hench, J.Wilson, F.Sugihora, E.Tsuji, M.Matsuura, S.Kin, T.Yamamoto, S.Mizokawa; J.Biomedical.Mater.Res.Part A, **51**, 37-46 **(2000)**.

[54] B.D.Cullity; 'Elements of X–ray Diffraction', Addison-Wesley, Reading, MA, **(1978)**.

[55] International Centre for Diffraction Data, file 40-393, $Ca_5(PO_4)_2SiO_4$ (Silicocarnotite, syn), **(1997)**.

[56] A.E.Porter, S.M.Rea, M.Galtrey, S.M.Best, Z.H.Barber; J.Mater.Sci., **39**, 1895-1898 **(2004)**.

[57] N.Hijon, M.V.Cabanas, J.Pena, M.Vallet-Regi; Acta Biomaterialia, **2(5)**, 567-574 **(2006)**.

[58] X.L.Tang, X.F.Xiao, R.F.Liu; Mater.Lett., **59**, 3841-3846 **(2005)**.

[59] P.Delvasto, A.Valverde, A.Ballester, J.M.Igual, J.A.Munoz, F.F.Gonzalez, M.L.Blazquez, C.García; Soil Biology & Biochemistry, **38**, 2645-2654 **(2006)**.

[60] C.Oliveira, P.Georgieva, F.Rocha, A.Ferreira, S.F.de Azevedo; Journal of Crystal Growth, **305**, 201-210 **(2007)**.

[61] E.S.Thian, J.Huang, M.E.Vickers, S.M.Best, Z.H.Barber, W.Bonfield; J.Mater.Sci., **41**, 709-717 **(2006)**.

[62] J.L.Xu, K.A.Khor, Z.L.Dong, Y.W.Gu, R.Kumar, P.Cheang; Materials Science and Engineering A, **374**, 101-108 **(2004)**.

[63] R.C.Rouse, P.J.Dunn; American Mineralogist, **67**, 90-96 **(1982)**.

[64] N.S.Chickerur, M.S.Tung, W.E.Brown; Calcif.Tissue Int., **32**, 55-62 **(1980)**.

[65] M.Aizawa, H.Ueno, K.Itatani, I.Okada; Journal of the European Ceramic Society, **26**, 501-507 **(2006)**.

[66] M.Palard, E.Eric Champion, S.Foucaud; Journal of Solid State Chemistry, **181**, 1950- 1960 **(2008)**.

[67] S.Sprio, A.Tampieri, E.Landi, M.Sandri, S.Martorana, G.Celotti, G.Logroscino; Materials Science and Engineering C, **28**, 179-187 **(2008)**.

[68] R.Murugan, S.Ramakrishna; Acta Biomaterialia, **2**, 201-206 **(2006)**.

[69] S.Raynaud, E.Champion, D.Bernache-Assollant, P.Thomas; Biomaterials, **23**, 1065-1072 **(2002)**.

[70] J.D.Russell, A.R.Fraser; In: 'Clay Mineralogy: Spectroscopic and Chemical Determinative Methods', Edited by M.J.Wilson, Chapman Hall, London, U.K., 11-67 **(1994)**.

[71] R.Z.LeGeros; Prog.Cryst.Growth.Charact., **4**, 1-45 **(1981)**.

[72] P.F.McMillan; In: Volatiles in Magmas, Reviews in Mi-neralogy, Edited by M.R.Caroll, J.R.Holloway; Mineral-ogical Society of America, Washington, D.C., **30**, 131-55 **(1994)**.

[73] D.E.Ellis, J.Terra, O.Warschkow, M.Jiang, G.B.Gonzalez, J.S.Okasinski, M.J.Bedzyk, A.M.Rossi, J.G.Eon; Phys.Chem.Chem.Phys., **8**, 967-976 **(2006)**.

[74] M.Markovic, B.O.Fowler, M.S.Tung; J.Res.Natl.Inst.Stand.Technol., **109**, 553-568 **(2004)**.

[75] E.E.Berry; J.Inorg.Nucl.Chem., **29**, 317-327 **(1967)**.

[76] C.B.Baddiel, E.E.Berry; Spectrochimica Acta, **22**, 1407-1461 **(1966)**.

[77] S.R.Kim, D.H.Riu, Y.J.Lee, Y.H.Kim; Key Eng.Mater., **85**, 218-220 **(2002)**.
[78] I.R.Gibson, S.M.Best, W.Bonfield; J.Biomed. Mater.Res., **44**, 422-428 **(1999)**.
[79] P.A.A.P.Marques, M.C.F.Magalhaes, R.N.Correia, M.Vallet-Regí; Key Eng.Mater., **192-195**, 247-250 **(2001)**.
[80] R.C.Tacker; American Mineralogist, **89**, 1411-1421 **(2004)**.
[81] A.Hadrich, A.Lautie, T.Mhiri; Spectrochimica Acta Part A, **57**, 1673-1681 **(2001)**.
[82] F.Freund, R.M.Knobel; J.C.S.Dalton, 1136-1140 **(1977)**.
[83] R.Astala, L.Calderin, X.Yin, M.J.Stott; Chem. Mater., **18(2)**, 413-422 **(2006)**.
[84] M.Hanke; Appl.Spectroscpy, **40**, 871-877 **(1986)**.
[85] F.McMillan, R.L.Remmele Jr.; Am.Mineral., **71**, 772-778 **(1986)**.
[86] M.Sitarz, M.Rokita, M.Handke; Ceramika, **66**, 243-249 **(2001)**.
[87] Y.Tanizawa, T.Suzuki; J.Chem.Soc.Faraday Trans, **91**, 3499-3500 **(1995)**.
[88] P.Yu, R.J.Kirkpatrick, B.Poe, P.F.McMillan, X.Cong; J.Am.Ceram.Soc., **82(3)**, 742-748 **(1999)**.
[89] M.M.Rashad, H.M.Baioumy, E.A.Abdel-Aal; Cryst.Res.Technol., **38(6)**, 433-439 **(2003)**.
[90] Th.Leventouri, C.E.Bunaciu, V.Perdikatsis; Biomaterials, **24**, 4205-4211 **(2003)**.
[91] D.Dunfield, M.Sayer, H.F.Shurvell; J.Phys.Chem.B, **109**, 19579-19583 **(2005)**.